

**MELT FRACTURE AND WALL SLIP CHARACTERISTICS OF HDPE
AND LLDPE**

Ms. Methavee Kwaengsobha

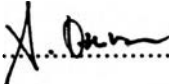
A Thesis Submitted in Partial Fulfillment of Requirements
for the Degree of Master of Science
The Petroleum and Petrochemical College
Chulalongkorn University
in Academic Partnership with
The University of Michigan, The University of Oklahoma
and Case Western Reserve University

1998

ISBN 974-638-478-3

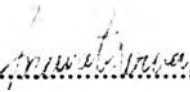
Thesis Title : Melt Fracture and Wall Slip Characteristics of HDPE
and LLDPE
By : Ms. Methavee Kwaengsobha
Program : Polymer Science
Thesis Advisors : Prof. Ronald G. Larson
Assoc. Prof. Anuvat Sirivat

Accepted by the Petroleum and Petrochemical College, Chulalongkorn
University, in the Partial Fulfillment of the Requirements for the Degree of
Master of Science.


..... Director of the College
(Prof. Somchai Osuwan)

Thesis Committee


.....
(Prof. Ronald G.Larson)


.....
(Assoc. Prof. Anuvat Sirivat)


.....
(Dr.Rathanawan Magaraphan)

ABSTRACT

962004 : POLYMER SCIENCE PROGRAM

KEY WORDS : Wall Slip / Stick-Slip Transition / Melt Fracture /
Extrapolation Length

Methavee Kwaengsobha : Melt Fracture and Wall Slip
Characteristics of HDPE and LLDPE. Thesis Advisors: Prof. Ronald G. Larson
and Assoc. Prof. Anuvat Sirivat, 170 pp. ISBN 974-638-478-3

We investigated the wall slip characteristics of HDPE and LLDPE polymer melts from the capillary extrusion. The wall slip magnitude of HDPE and LLDPE was found to increase with temperature but to decrease with molecular weight. The slip velocity depends on the wall shear stress according to the power law $V_s = A\tau_w^m$, where A depends on temperature, molecular structure, and molecular weight. The scaling exponent m depends only on molecular structure and molecular weight.

The extrapolation length was used to characterize the slip velocity following the theory of Brochard and de Gennes. Our results indicate that at low temperature and with a high molecular weight, the entanglement state was observed because the grafted chains which are attached to the wall surface effectively entangle with the mobile chains. On the other hand, at high temperature, the marginal state was observed because some grafted chains have been fully extended resulting in a smaller entanglement loci density. The extrapolation length obeys the linear law $b = CV_s$ where C depends slightly on temperature but strongly on molecular weight. C was found to be equal to η'_0/τ^* where η'_0 is the zero shear rate viscosity and τ^* is onset shear stress for slip, consistent with the theory of Brochard and de Gennes in the marginal regime. No rouse regime was observed in this experiment.

บทคัดย่อ

เมธาวิ แขวงโสภา: การศึกษาผิวขรุขระของพลาสติกและอัตราการไหลที่ไม่นำ
 เสมอบนชิ้นส่วนของพลาสติกที่ถูกรีดจากท่อกลมของพอลิเอทิลีนชนิดความหนาแน่นสูงและ พอลิเอทิลีนชนิดความหนาแน่นเชิงเส้นต่ำ (Melt Fracture and Wall Slip Characteristics of HDPE and LLDPE) อ.ที่ปรึกษา : Prof. Ronald G. Larson และ รศ. ดร. อนุวัฒน์ ศิริวัฒน์
 170 หน้า ISBN 974-638-478-3

วิทยานิพนธ์นี้ เสนอการค้นคว้าเกี่ยวกับการเกิดผิวขรุขระ และอัตราการไหลที่
 ไม่นำเสมอบนชิ้นส่วนพลาสติกที่เกิดจากกระบวนการรีดจากท่อกลม จากการทดลองพบว่า อัตรา
 การไหลที่ไม่นำเสมอของสารโพลิเมอร์ จะเพิ่มขึ้นตามอุณหภูมิ แต่จะลดลงตามน้ำหนัก
 โมเลกุลของโพลิเมอร์ นอกจากนี้ ยังขึ้นอยู่กับค่าความเค้นยกกำลังด้วย

การลากระยะทางของอัตราการไหลที่ไม่นำเสมอจากผิวท่อกลมไปเป็นศูนย์กลาง
 ได้นำมาใช้ในการศึกษาลักษณะเฉพาะของอัตราการไหล ตามทฤษฎีของ Brochard และ de
 Gennes ซึ่งจากการทดลองพบว่า ที่อุณหภูมิต่ำ และพอลิเมอร์มีน้ำหนักโมเลกุลสูง จะสังเกตพบ
 สภาวะที่สายโซ่พอลิเมอร์มีการพันกัน เนื่องจากสายโซ่พอลิเมอร์ที่ติดอยู่กับผนังท่อสามารถที่จะ
 พันกันกับสายโซ่พอลิเมอร์ ที่เคลื่อนที่ได้ นอกจากนี้ ยังพบว่าที่อุณหภูมิสูง จะสังเกตพบสภาวะที่
 อัตราการไหลที่ไม่นำเสมอของพอลิเมอร์จะมีความสัมพันธ์เชิงเส้นกับการลากระยะทางของ
 อัตราการไหลที่ไม่นำเสมอของพอลิเมอร์ เนื่องจากสายโซ่พอลิเมอร์บางส่วนที่ติดกับผนังท่อมี
 การยืดตัวออกทำให้ความหนาแน่นในการพันกันของพอลิเมอร์ลดลง และยังมีความสัมพันธ์กับ
 ความหนืดของพอลิเมอร์ที่ความเร็วเป็นศูนย์กลาง และความเค้นเริ่มต้นของการเกิดอัตราการไหล
 อย่างไรก็ดีในการทดลองนี้ไม่พบสภาวะที่พอลิเมอร์มีการเคลื่อนที่อย่างอิสระ

ACKNOWLEDGMENTS

The author greatly appreciates the efforts of her research advisors, Professor Ronald G. Larson, Department of Chemical Engineering, University of Michigan and Associate Professor Anuvat Sirivat of the Petroleum and Petrochemical College, Chulalongkorn University for their constructive criticisms, suggestions and proof-reading of this manuscript. She would like to give thanks to Dr. Ratthanawan Magaraphan for being a thesis committee member.

She would like to thank the Siam Chemical Trading Co., Ltd and Thai Petrochemical Industry Public Co., Ltd. for the raw materials and performing the density measurements, melt flow measurements and the size exclusion chromatography measurements.

The author also thanks all of her friends and the staff of the PPC who encouraged her in carrying out all the experiment and this thesis writing. Finally, she is deeply indebted to her presents and aunts for their love, understanding, generous encouragements, and for being a constant source of her inspiration.

TABLE OF CONTENTS

	PAGE
Title Page	i
Abstract	iii
Acknowledgments	v
List of Tables	ix
List of Figures	xi
CHAPTER	
I	INTRODUCTION
1.1 Extrudate Distortion	2
1.1.1 Sharkskin	2
1.1.2 Oscillating Flow	2
1.1.3 Wavy Fracture	3
1.2 Wall Slip	3
1.3 Extrapolation Length	5
1.4 Previous Studies	6
1.5 Research Objectives	10
II	EXPERIMENTAL SECTION
2.1 Materials	11
2.1.1 High Density Polyethylene	11
2.1.2 Linear Low Density Polyethylene	11
2.1.3 Medium Density Polyethylene	12

CHAPTER	PAGE
2.2 Characterizations	12
2.2.1 Melt Flow Index Meter	13
2.2.2 Gel Permeation Chromatography	13
2.2.3 Density Measurement	13
2.2.4 Zoom stereo Microscope	13
2.3 Capillary Rheometer	14
2.3.1 Instrument	14
2.3.2 Procedure	14
2.3.3 Calculation	15
2.4 Parallel Plate Rheometer	20
2.4.1 Instrument	20
2.4.2 Procedure	21
2.4.3 Data Analysis	21
III RESULTS AND DISCUSSION	23
3.1 Flow Curve	23
3.2 Surface Texture	27
3.3 Rheological Characterizations	33
3.3.1 The storage modulus (G') and the loss modulus (G'')	34
3.3.2 Master Curve	41
3.3.3 Cox-Merx Rule	45
3.3.4 Viscosity	54
3.3.5 The stress at the onset of the slip velocity	64
3.4 Effect of Temperature on Slip	73
3.4.1 Slip Velocity	73

CHAPTER	PAGE
3.4.2 Extrapolation Length	80
3.5 Effect of Molecular Weight	86
3.5.1 Slip Velocity	86
3.5.2 Extrapolation Length	90
3.6 Scaling	94
3.6.1 Effect of Temperature	94
3.6.2 Effect of Molecular Weight	96
IV CONCLUSIONS	98
REFERENCES	99
APPENDICES	103
CURRICULUM VITAE	182

LIST OF TABLES

TABLE		PAGE
2.1.1	Physical properties of HDPE as given by manufacturer	11
2.1.2	Physical properties of LLDPE as given by manufacturer	12
2.1.3	Physical properties of MDPE as given by manufacturer	12
2.3	Capillary dies features	14
3.2.1	Stereomicroscope photography of the melt fracture of LLDPE (L2009F) at temperature of 190°C	30
3.2.2	The critical wall shear stress ($\tau_{w,c}$) and the strain rate (γ_a) for LLDPE (L2009F and M3204RU) and HDPE (H5690S and H6205JU) at temperature of 190°C	31
3.2.3	The critical wall shear stress ($\tau_{w,c}$) and the strain rate (γ_a) for LLDPE (L2020F) and HDPE (H5690S) at temperatures between 150-230°C	32
3.3.1	Physical properties of all materials studied	33
3.3.2	The values of G^0_N , the zero complex viscosity, η^*_0 , the zero shear viscosity, $\eta'_{0,c}$, and the stress at the onset of the slip velocity, τ^* , for LLDPE (L2020F) and HDPE (H5690S) at temperatures between 150-230°C	71

TABLE	PAGE	
3.3.3	The values of G^0_N , the zero complex viscosity, η^*_0 , the zero shear viscosity, η'_0 , and the stress at the onset of the slip velocity, τ^* , for LLDPE (L2009F, L2020F and M3204RU) and HDPE (H5604F, H5690S and H6205JU) at temperature of 190°C. of different molecular weights	72
3.4.1	The values of power law parameters A, m and the onset of wall shear stress, τ^* , at temperatures between 150-230°C for LLDPE (L2020F) and HDPE (H5690S)	79
3.4.2	The values of the parameter C, at different temperatures for LLDPE (L2020F) and HDPE (H5690S)	86
3.5.1	The values of power law parameters A and m at the temperature of 190°C for LLDPE and HDPE of different molecular weights	89
3.5.2	The values of the parameter C for LLDPE and HDPE of different molecular weights	94

LIST OF FIGURES

FIGURE	PAGE
<p>1.1(a) Plot of velocity field at the stick-slip transition in the capillar corresponding to the “stick” state, with sufficient chain entanglement denoted by the dots and with zero slip velocity</p> <p>(b) Plot of velocity fiend at the transition corresponding to the “slip” state, with exaggerated depiction of zero chain entangments in the interfacial layer and a much larger apparent flow throughput due to a finite slip velocity</p>	4
1.2 Plot of three regimes of slip velocity in the plot between the extrapolation length, b versus the slip velocity, V_s	6
2.1 Plot of viscoty vs. the apparent strain rate	17
3.1 Plot of wall shear stress, τ_w , as a function of the apparent strain rate, γ_a , for LLDPE(L2009F) at temperature of 190 °C	24
3.2 Plot of wall shear stress, τ_w , as a function of the apparent strain rate, γ_a , for LLDPE(2020F) at temperature of 190 °C	25
3.1 Plot of wall shear stress, τ_w , as a function of the apparent strain rate, γ_w , for MDPE (M3204RU) at temperature of 190 °C	25

FIGURE	PAGE
3.4 Plot of wall shear stress, τ_w , as a function of the apparent strain rate, γ_a , for HDPE (H5690S) at temperature of 190 °C	26
3.5 Plot of wall shear stress, τ_w , as a function of the apparent strain rate, γ_a , for HDPE (H5604F) at temperature of 190 °C	26
3.6 Plot of wall shear stress, τ_w , as a function of the temperature strain rate, γ_a , for HDPE (H6205JU) at the temperature of 190 °C	27
3.7 Stereomicroscope photography of the smooth extrudate of LLDPE (L2009F) at temperature of 190 °C	28
3.8 Stereomicroscope photography of the sharkskin extrudate of LLDPE (L2009F) at temperature of 190 °C	29
3.9 Stereomicroscope photography of the alternating surfaces between smooth and sharkskin of LLDPE (L2009F) at temperature of 190 °C	29
3.10 Stereomicroscope photography of the melt fracture of LLDPE (L2009F) at temperature of 190 °C	30
3.11 Plot of storage modulus, G' , as a function of the frequency, ω , of LLDPE (L2009F) melts at temperatures	35
3.12 Plot of storage modulus, G' , as a function of the frequency, ω , of LLDPE (L2009F) melts at different temperatures	35
3.13 Plot of storage modulus, G' , as a function of the frequency, ω , of LLDPE (M3204RU) melts at different temperatures	36
3.14 Plot of storage modulus, G' , as a function of the frequency, ω , of HDPE (H5604F) melts at different temperatures	36

FIGURE	PAGE
3.15 Plot of storage modulus, G' , as a function of the frequency, ω , of HDPE (H5690S) melts at different temperatures	37
3.16 Plot of storage modulus, G' , as a function of the frequency, ω , of HDPE (H6205JU) melts at different temperatures	37
3.17 Plot of storage modulus, G'' , as a function of the frequency, ω , of LLDPE (L2009F) melts at different temperatures	38
3.18 Plot of storage modulus, G'' , as a function of frequency, ω , of LLDPE (L2020F) melts at different temperatures	38
3.19 Plot of storage modulus, G'' , as a function of frequency, ω , of LLDPE (M3204RU) melts at different temperatures	39
3.20 Plot of storage modulus, G'' , as a function of the frequency, ω , of HDPE (H5604F) melts at different temperatures	39
3.21 Plot of storage modulus, G'' , as a function of the frequency, ω , of HDPE (H5690S) melts at different temperatures	40
3.22 Plot of storage modulus, G'' , as a function of the frequency, ω , of HDPE (H6205JU) melts at different temperatures	40
3.23 Master curve of LLDPE (L2009F) melts at reference temperature of 190 °C	42
3.24 Master curve of LLDPE (L202F) melts at reference temperature of 190 °C	42
3.25 Master curve of LLDPE (M3204RU) melts at reference temperature of 190 °C	43
3.26 Master curve of HDPE (H5604F) melts at reference temperature of 190 °C	43
3.27 Master curve of HDPE (H5690S) melts at reference temperature of 190 °C	44

FIGURE	PAGE
3.28 Master curve of HDPE (H6205JU) melts at reference temperature of 190 °C	44
3.29 Plot of viscosity as a function of the apparent strain rate and frequency of LLDPE (L202F) melts by Cox-Merz rule at temperature of 150 °C	46
3.30 Plot of viscosity as a function of the apparent strain rate and frequency of LLDPE (L2020F) melts by Cox-Merz rule at temperature of 170 °C	46
3.31 Plot of viscosity as a function of the apparent strain rate and frequency of LLDPE melts (L2020F) melts by Cox-Merz at temperature of 190 °C	47
3.32 Plot of viscosity as a function of the apparent strain rate and frequency of LLDPE (L2020F) melts by Cox-Merz rule at temperature of 210 °C	47
3.33 Plot of viscosity as a function of the apparent strain rate and frequency of HDPE (H5690S) melts by Cox-Merz rule at temperature of 230 °C	48
3.34 Plot of viscosity as a function of the apparent strain rate and frequency of HDPE (H5690S) melts by Cox-Merz rule at temperature of 150 °C	48
3.35 Plot of viscosity as a function of the apparent strain rate and frequency of HDPE (H5690S) melts by Cox-Merz rule at temperature of 170 °C	49
3.36 Plot of viscosity as a function of the apparent strain rate and frequency of HDPE (H5690S) melts by Cox-Merz rule at temperature of 190 °C	49

FIGURE	PAGE
3.37 Plot of viscosity as a function of the apparent strain rate and frequency of HDPE (H5690S) melts by Cox-Merz rule at temperature of 210 °C	50
3.38 Plot of viscosity as a function of the apparent strain rate and frequency of HDPE (H5690S) melts by Cox-Merz rule at temperature of 230 °C	50
3.39 Plot of viscosity as a function of the apparent strain rate and frequency of LLDPE (L2009F) melts by Cox-Merz rule at temperature of 190 °C	51
3.40 The viscosity as a function of the apparent strain rate and frequency of LLDPE (L2020F) melts by Cox-Merz rule at temperature of 190 °C	52
3.41 Plot of viscosity as a function of the apparent strain rate and frequency of LLDPE (M3204RU) melts by Cox-Merz rule at temperature of 190 °C	52
3.42 Plot of viscosity as a function of the apparent strain rate and frequency of HDPE (H5604F) melts by Cox-Merz rule at temperature of 190 °C	53
3.43 Plot of viscosity as a function of the apparent strain rate and frequency of HDPE (H5690S) melts by Cox-Merz rule at temperature of 190 °C	53
3.44 Plot of viscosity as a function of the apparent strain rate and frequency of HDPE (H6205JU) melts by Cox-Merz rule at temperature of 190 °C	54
3.45 Plot of viscosity as a function of the frequency of LLDPE (L2020F) melts at temperature of 150 °C	55

FIGURE	PAGE
3.46 Plot of viscosity as a function of the frequency of LLDPE (L2020F) melts at temperature of 170 °C	56
3.47 Plot of viscosity as a function of the frequency of LLDPE (L2020F) melts at temperature of 190 °C	56
3.48 Plot of viscosity as a function of the frequency of LLDPE (L2020F) melts at temperature of 210 °C	57
3.49 Plot of viscosity as a function of the frequency of LLDPE (L2020F) melts at temperature of 230 °C	57
3.50 Plot of viscosity as a function of the frequency of HDPE (H5690S) melts at temperature of 150 °C	58
3.51 Plot of viscosity as a function of the frequency of HDPE (H5690S) melts at temperature of 170 °C	58
3.52 Plot of viscosity as a function of the frequency of HDPE (H5690) melts at temperature of 190 °C	59
3.53 Plot of viscosity as a function of the frequency of HDPE (H5690S) melts at temperature of 210 °C	59
3.54 Plot of viscosity as a function of the frequency of HDPE (H5690S) melts at temperature of 230 °C	60
3.55 Plot of viscosity as a function of the frequency of LLDPE (L2009F) melts at temperature of 190 °C	61
3.56 Plot of viscosity as a function of the frequency of LLDPE (L2020F) melts at temperature of 190 °C	61
3.57 Plot of viscosity as a function of the frequency of LLDPE (M3204RU) melts at temperature of 190 °C	62
3.58 Plot of viscosity as a function of the frequency of HDPE (H5604F) melts at temperature of 190 °C	62

FIGURE	PAGE
3.59 Plot of viscosity as a function of the frequency of HDPE (H5690S) melts at temperature of 190 °C	63
3.60 Plot of viscosity as a function of the frequency of HDPE (H6205J) melts at temperature of 190 °C	63
3.61 Plot of slip velocity, V_S , as a function of the wall shear stress, τ_W , for LLDPE (L2020F) melts at temperature of 170 °C	64
3.62 Plot of slip velocity, V_S , as a function of the wall shear stress, τ_W , for LLDPE (L2020F) melts at temperature of 190 °C	65
3.63 Plot of slip velocity, V_S , as a function of the wall shear stress, τ_W , for LLDPE (L2020F) melts at temperature of 210 °C	65
3.64 Plot of slip velocity, V_S , as a function of the wall shear stress, τ_W for LLDPE (L2020F) melts at temperature of 230 °C	66
3.65 Plot of slip velocity, V_S , as a function of the wall shear stress, τ_W , for HDPE(H5690S) melts at temperature of 190 °C	66
3.66 Plot of slip velocity, V_S , as a function of the wall shear stress, τ_W , for HDPE(H5690S) melts at temperature of 210 °C	67
3.67 Plot of slip velocity, V_S , as a function of the wall shear stress, τ_W , for HDPE (H5690S) melts at temperature of 230 °C	67

FIGURE	PAGE
3.68 Plot of slip velocity, V_s , as a function of the wall shear stress, τ_w , for LLDPE (L2009F) melts at temperature of 190 °C	68
3.69 Plot of slip velocity, V_s , as a function of the wall shear stress, τ_w , for LLDPE (L2020F) melts at temperature of 190 °C	69
3.70 Plot of slip velocity, V_s , as a function of the wall shear stress, τ_w , for LLDPE (M3204RU) melts at temperature of 190 °C	69
3.71 Plot of slip velocity, V_s , as a function of the wall shear stress, τ_w , for HDPE (H5690S) melts at temperature of 190 °C	70
3.72 Plot of slip velocity, V_s , as a function of the wall shear stress, τ_w for HDPE (H6205JU) melts at temperature of 190 °C	70
3.73 Plot of apparent strain rate, γ_a , as a function of one over diameter of a capillary, $1/d_c$, for HDPE (H5690S) at temperature of 190 °C	73
3.74 Plot of slip velocity, V_s , as a function of the wall shear stress, τ_w of LLDPE (L2020F) at temperature of 150-230 °C	74
3.75 (a) Plot of slip velocity, V_s , as a function of the wall shear stress, τ_w , for HDPE (H5690S) at temperature of 150 °C, 190 °C and 230 °C	75

FIGURE	PAGE
(b) Plot of slip velocity, V_s , as a function of the wall shear stress, τ_w , for HDPE (H5690S) at temperature of 170 °C and 210 °C	75
3.76 Plot of slip velocity, V_s , as a function of the wall shear stress, τ_w , on log-log plot of LLDPE (L2020F) at temperatures of 150-230 °C	77
3.77 (a) Plot of slip velocity, V_s , as a function of the wall shear stress, τ_w , on log-log plot of HDPE (H5690S) at temperatures of 150 °C, 190 °C and 230 °C	77
3.77(b) Plot of slip velocity, V_s , as a function of the wall shear stress, τ_w , on log-log plot of HDPE (H5690S) at temperatures of 170 °C and 210 °C	78
3.78 Plot of extrapolation length, b , as a function of the slip velocity, V_s , of LLDPE (L2020F) at temperature of 150 °C	81
3.79 Plot of extrapolation length, b , as a function of the slip velocity, V_s , of LLDPE (L2020F) at temperature of 170 °C	82
3.80 Plot of extrapolation length, b , as a function of the slip velocity, V_s , of LLDPE (L2020F) at temperature of 190 °C	82
3.81 Plot of extrapolation length, b , as a function of the slip velocity, V_s , of LLDPE (L2020F) at temperature of 210 °C	83

FIGURE	PAGE
3.82 Plot of extrapolation length, b , as a function of the slip velocity, V_s , of LLDPE (L2020F) at temperature of 230 °C	83
3.83 Plot of extrapolation length, b , as a function of the slip velocity, V_s , of HDPE (H5690S) at temperature of 170 °C	84
3.84 Plot of extrapolation length, b , as a function of the slip velocity, V_s , of HDPE (H5690S) at temperature of 190 °C	84
3.85 Plot of extrapolation length, b , as a function of the slip velocity, V_s of HDPE (H5690S) at temperature of 210 °C	85
3.86 Plot of extrapolation length, b , as a function of the slip velocity, V_s , of HDPE (H5690S) at temperature of 230 °C	85
3.87 Plot of slip velocity, V_s , as a function of the wall shear stress, τ_w , for LLDPE (L2020F) of different molecular weights	87
3.88 Plot of slip velocity, V_s , as a function of the wall shear stress, τ_w , for HDPE (H5690S) of different molecular weights	87
3.89 Plot of slip velocity, V_s , as a function of the wall shear stress, τ_w , on log-log plot of LLDPE (L2020F) of different molecular weights	88

FIGURE	PAGE
3.90 Plot of slip velocity, V_S , as a function of the wall shear stress, τ_w , on log-log plot of HDPE (H5690S) of different molecular weights	89
3.91 Plot of extrapolation length, b , as a function of the slip velocity, V_S , at temperature of 190 °C for LLDPE (L2009F)	91
3.92 Plot of extrapolation length, b , as a function of the slip velocity, V_S , at temperature of 190 °C for LLDPE (L2020F) Plot of extrapolation length, b , as a function of the slip velocity, V_S , at temperature of 190 °C for LLDPE (L2020F)	91
3.93 Plot of extrapolation length, b , as a function of the slip velocity, V_S , at temperature of 190 °C for LLDPE (L2020F) Plot of extrapolation length, b , as a function of the slip velocity, V_S , at temperature of 190 °C for LLDPE (M3204RU)	92
3.94 Plot of extrapolation length, b , as a function of the slip velocity, V_S , at temperature of 190 °C for HDPE (H5604F)	92
3.95 Plot of extrapolation length, b , as a function of the slip velocity, V_S , at temperature of 190 °C for HDPE (H5690S)	93
3.96 Plot of extrapolation length, b , as a function of the slip velocity, V_S , at temperature of 190 °C for HDPE (H6205JU)	93

FIGURE	PAGE
3.97 Plot of extrapolation length, b , vs. $(\eta'_0 V_S)/\tau^*$ for LLDPE (L2020F) melts at temperatures between 170-230 °C	95
3.98 Plot of extrapolation length, b , vs. $(\eta'_0 V_S)/\tau^*$ for HDPE (H5690S) melts at temperatures between 190-230 °C	96
3.99 Plot of extrapolation length, b , vs. $(\eta'_0 V_S)/\tau^*$ for LLDPE (L2009F, L2020F and M3204RU) at temperature of 190 °C	97
3.100 Plot of extrapolation length, b , vs. $(\eta'_0 V_S)/\tau^*$ for HDPE (H5690S and H6205JU) at temperature 190 °C	97